

## Regulatory factor linked to late-onset diabetes?

Maintenance of glucose balance in mammals depends on the production of insulin by the  $\beta$ -cells of the pancreas, in response to raised concentrations of blood glucose. In humans suffering from non-insulin-dependent diabetes (NIDDM),  $\beta$ -cell failure follows chronic resistance to insulin-stimulated glucose uptake and causes the development of hyperglycaemia<sup>1</sup>. NIDDM shows a polygenic inheritance pattern in most cases<sup>2</sup>: defined genetic defects that have little effect on their own, in combination induce diabetes by epistatic interactions<sup>3</sup>. Here we show that mice heterozygous for the gene *pdx-1*, which encodes a transcription factor for the insulin gene and regulates pancreatic development, have impaired glucose tolerance. This pancreatic nuclear regulatory factor is required for glucose homeostasis even when the pancreas is morphologically normal.

The *pdx-1*-encoded homeodomain protein in mammals (STF-1, IPF-1, IDX-1)<sup>4-6</sup> was isolated as a transcriptional regulator of insulin and somatostatin<sup>7-9</sup>. The protein was first detected in the embryonic pancreatic and duodenal endoderm. But in the pancreas, *pdx-1* expression becomes progressively restricted to islets, where it is produced in more than 90% of  $\beta$ -cells, and in substantially fewer  $\delta$ -cells (15%) and  $\alpha$ -cells (3%)<sup>10,11</sup>.

Mice that are heterozygous (+/-) for *pdx-1* develop normally, but in *pdx-1* homozygotes (-/-), the branching outgrowth of the pancreas that usually occurs is arrested at an early stage<sup>11,12</sup>. The relevance of these findings is underscored by a description of a human phenotype lacking a pancreas and associated with a mutation in the *pdx-1* gene<sup>13,14</sup>. Maturity-onset diabetes occurred in humans heterozygous for this mutation<sup>13</sup>; this prompted us to examine whether *pdx-1* is important for glucose homeostasis in an adult mouse model.

We fasted *pdx-1* wild-type and +/- mice for 14–16 hours and injected them intraperitoneally with 20% glucose (2 grams per kilogram body weight). The blood glucose levels of the wild type underwent a threefold increase within 15 minutes but returned to baseline two hours later (Fig. 1a). By contrast, +/- mice showed a 7–10-tenfold increase in blood glucose levels after 30 minutes. These mice remained hyperglycaemic even after 2 hours (Fig. 1a).

The levels of plasma insulin following glucose administration (not shown) did

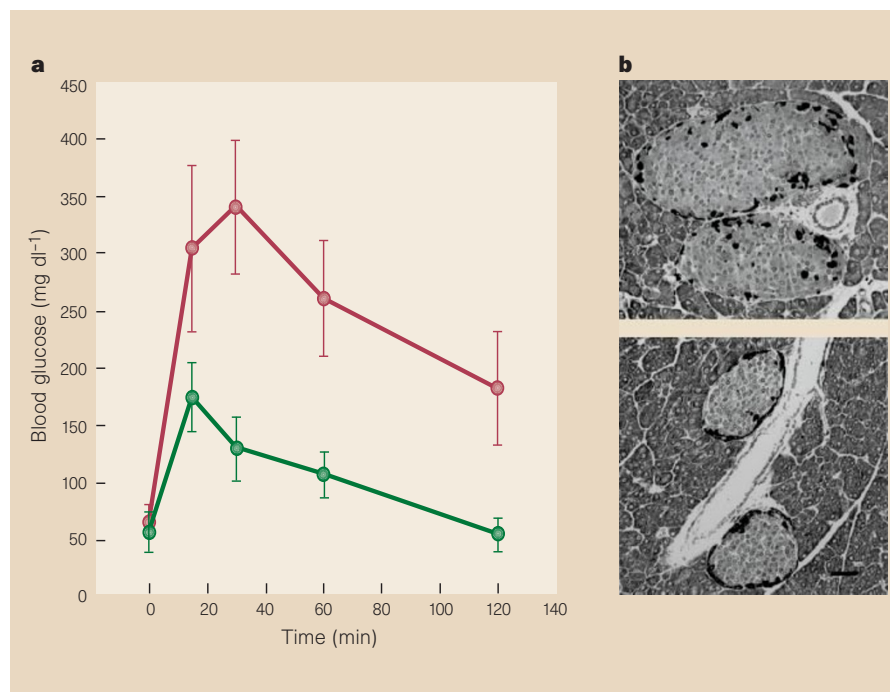


**Figure 1** Comparison of wild-type and *pdx-1*-deficient mice. **a**, Glucose tolerance tests on black Swiss mice that are either heterozygous for *pdx-1* (+/-, red) or wild type (green). Mean blood glucose levels over time are shown with standard error ( $n = 8$  for wild-type mice,  $n = 11$  for +/- mice). Animals were fasted for 14–16 hours before testing. Blood glucose levels were monitored with a glucometer. **b**, Representative islets from 15-week-old wild-type (top) and +/- (bottom) mice. Islets were immunostained with combined antibodies raised against glucagon, somatostatin and pancreatic polypeptide to show the mantle of islet non- $\beta$ -cells around the core of unstained  $\beta$ -cells. Magnification bar, 50  $\mu$ m.

not differ appreciably between wild-type and +/- animals, but these insulin levels were inappropriately low for the degree of hyperglycaemia observed in the +/- mice.

In histological evaluation, the pancreatic islets from the +/- mice appeared somewhat smaller, with a thicker mantle devoid of  $\beta$ -cells, than those of the wild type (Fig. 1b). The mass of  $\beta$ -cells was reduced, but to an extent that was not significant (wild-type mice: 2.80 milligrams  $\pm$  0.44;  $n = 8$ ; +/- mice: 1.76 milligrams  $\pm$  0.13;  $n = 4$ ). However, the mass of non- $\beta$ -cells was almost doubled in +/- compared with wild-type mice (wild-type mice: 0.47 mg  $\pm$  0.06; +/- mice: 0.82 mg  $\pm$  0.10). This suggests that a deficiency in the *pdx-1* gene may skew the islet cell lineages towards developing into non- $\beta$  cells.

Our results support the idea that, as well as acting as a regulatory protein for pancreatic development, the protein encoded by *pdx-1* is required for glucose homeostasis in the adult pancreas. Thus a deficiency in *pdx-1* may predispose certain individuals to the development of late-onset diabetes, particularly in the context of other genetic mutations within the insulin-signalling cascade.

**Sanjoy Dutta, Susan Bonner-Weir, Marc Montminy**

Joslin Diabetes Center, Department of Cell Biology  
Harvard Medical School, Boston,  
Massachusetts 02215, USA

**Christopher Wright**

Vanderbilt University School of Medicine,  
Department of Cell Biology, Nashville,  
Tennessee 37232-2175, USA

1. Ciaraldi, T. P., Abrams, L., Nikoulina, S., Mudaliar, S. & Henry, R. R. *J. Clin. Invest.* **96**, 2820–2827 (1995).
2. Sacks, D. B. & McDonald, J. M. *Am. J. Clin. Pathol.* **105**, 149–156 (1996).
3. Bruning, J. *et al. Cell* **88**, 561–572 (1997).
4. Leonard, J. *et al. Mol. Endocrinol.* **7**, 1275–1283 (1993).
5. Miller, C. P., McGhee, R. E. Jr & Habener, J. F. *EMBO J.* **13**, 1145–1156 (1994).
6. Ohlsson, H., Karlsson, K. & Edlund, T. *EMBO J.* **12**, 4251–4259 (1993).
7. Peers, B., Leonard, J., Sharma, S., Teitelman, G. & Montminy, M. R. *Mol. Endocrinol.* **8**, 1798–1806 (1994).
8. Peers, B., Sharma, S., Johnson, T., Kamps, M. & Montminy, M. *Mol. Cell. Biol.* **15**, 7091–7097 (1995).
9. Serup, P. *et al. Biochem. J.* **310**, 997–1003 (1995).
10. Guz, Y. *et al. Development* **121**, 11–18 (1995).
11. Offield, M. F. *et al. Development* **122**, 983–995 (1996).
12. Jonsson, J., Carlsson, L., Edlund, T. & Edlund, H. *Nature* **371**, 606–609 (1994).
13. Stoffers, D. A., Zinkin, N. T., Stanojevic, V., Clarke, W. L. & Habener, J. F. *Nature Genet.* **15**, 106–110 (1997).
14. Stoffers, D. A., Ferrer, J., Clarke, W. J. & Habener, J. F. *Nature Genet.* **17**, 138–139 (1997).

### correction

In the Scientific Correspondence article entitled "Inhibition of ICE slows ALS in mice" by R. M. Friedlander, R. H. Brown, V. Gagliardini, J. Wang and J. Yuan (*Nature* **388**, 31; 1997), the mouse strain used was G93A (rather than G93R as published).

# Inhibition of ICE slows ALS in mice

Amiotrophic lateral sclerosis (ALS) is a progressive age-dependent disease involving degeneration of motor neurons in the brain, brainstem and spinal cord. ALS is universally fatal, with the median survival of patients being five years from diagnosis. In a transgenic mouse model of ALS, we now show that a dominant negative inhibitor of a cell-death gene, the interleukin-1 $\beta$ -converting enzyme (ICE), significantly slows the symptomatic progression of ALS.

ALS exists in both sporadic and familial forms. Certain familial forms are caused by mutations in the Cu/Zn superoxide dismutase (SOD-1) gene<sup>1</sup>. Transgenic mice expressing mutant SOD-1 genes develop an age-dependent progressive motor weakness similar to human ALS<sup>2</sup>. Although little is known about the mechanism of cell death in ALS, downregulation of SOD-1 activity using antisense SOD-1 DNA *in vitro* has been shown to promote apoptosis in a neuronal cell line<sup>3</sup>. Cell death in this model was mediated in part by the activation of ICE and by binding of endogenously produced mature interleukin-1 $\beta$  (IL-1 $\beta$ ) to its receptor<sup>4</sup>.

We have previously shown that endogenous mature IL-1 $\beta$ , produced by activation of ICE, is important in a variety of cell-death models<sup>5</sup>. We recently reported a transgenic mouse expressing a dominant negative inhibitor of ICE, which has the active-site cysteine substituted for a glycine, in neurons under the control of a neuronal specific enolase promoter (NSE-M17Z)<sup>6</sup>. Developmental neuronal cell death does not seem to be inhibited in these transgenic mice, as the brain is of normal size, they exhibit normal

**Table 1 Timing of disease onset and mortality**

	Mutant		P
	SOD (n=24)	SOD/M17Z (n=22)	
Onset	237.7 $\pm$ 4.4	243.0 $\pm$ 5.6	0.464
Length	11.7 $\pm$ 1.6	27.0 $\pm$ 3.5	0.0002*
Mortality	249.3 $\pm$ 3.8	270.0 $\pm$ 7.0	0.0115*

Disease onset, length and mortality are listed as mean  $\pm$  s.e.m. days, illustrating the delay in the mortality of SOD(G93R) transgenic mice by expression of a dominant negative inhibitor of ICE. Asterisks indicate a significant difference (unpaired t-test, two-tailed).

behaviour, and have equivalent numbers of neurons in the facial motor nucleus as the wild-type control mice<sup>6</sup>. This contrasts with the NSE-Bcl-2 transgenic mice which have larger brains and more neurons<sup>7</sup>.

To determine whether inhibition of ICE activity *in vivo* might halt the progression of the ALS-like syndrome in mice expressing mutant SOD-1, we crossed five female NSE-M17Z mice from one transgenic founder mouse with one mutant SOD(G93R) male mouse. We determined the genotypes of the progeny from these crosses using the polymerase chain reaction (PCR) to find carriers of the mutant ICE and SOD transgenes, and monitored littermates of SOD(G93R) mice and those with both SOD(G93R) and mutant ICE for the times of disease onset and death. The onset of the disease was scored as the date of the first observation of significantly slower gait and/or limb paralysis. Mortality was scored as the date of death or the inability of the mouse to right itself in 30 s (scorers were unaware of the genotypes of the mice or their birth dates).

Although the timing of disease onset in

the mutant SOD and mutant SOD/ mutant ICE (M17Z) transgenic mice is not different, the double-transgenic mice survive significantly longer from the onset of the disease (27 days) than the mutant SOD mice (11.7 days) (Table 1). Therefore, expression of the dominant negative inhibitor of ICE in neurons of mutant SOD mice is able to slow the symptomatic progression of this disease and delay mortality. Our results indicate that ICE-like proteases might affect disease progression in this ALS mouse model and suggest that ICE inhibitors may be of value in the treatment of ALS in humans.

**Robert M. Friedlander**

Neurosurgical Service, Department of Surgery, Massachusetts General Hospital, Harvard Medical School, Boston, Massachusetts 02114, USA

**Robert H. Brown**

Day Neuromuscular Research Laboratory, Massachusetts General Hospital, Charlestown, Massachusetts 02129, USA

**Valeria Gagliardini, Joy Wang, Junying Yuan**

Cardiovascular Research Center, Department of Medicine, Massachusetts General Hospital, Harvard Medical School, Charlestown, Massachusetts 02129, USA  
e-mail: jyuan@bcmp.med.harvard.edu

- Rosen, D. R. *et al.* *Nature* **362**, 59–62 (1993).
- Gurney, M. E. *et al.* *Science* **264**, 1772–1775 (1994).
- Rothstein, J. D., Bristol, L. A., Hosler, B., Brown, R. H. Jr & Kuncel, R. W. *Proc. Natl Acad. Sci. USA* **91**, 4155–4159 (1994).
- Troy, C. M. *et al.* *Proc. Natl Acad. Sci. USA* **93**, 5635–5640 (1996).
- Friedlander, R. M., Gagliardini, V., Rotello, R. J. & Yuan, J. *J. Exp. Med.* **184**, 717–724 (1996).
- Friedlander, R. M. *et al.* *J. Exp. Med.* **185**, 933–940 (1997).
- Martinou, J.-C. *et al.* *Neuron* **13**, 1017–1030 (1994).

## Electronic properties of carbon toroids

In a recent Scientific Correspondence, Liu *et al.*<sup>1</sup> reported observing carbon toroids. They suggested that these objects could be considered as quantum wires and that they would exhibit interesting transport properties. Here I provide theoretical support for this proposition.

The ring currents that flow in aromatic molecules in response to the application of a magnetic field are often likened to electrical conductivity<sup>2,3</sup>, so it is interesting to study the magnetic properties of the carbon toroids. I use as a test case the calculated structure of the C<sub>576</sub> toroid (ref. 4; and B. I. Dunlap and F. Negri, unpublished). This object is of C<sub>6v</sub> symmetry and resembles an inflated benzene molecule (Fig. 1). The structure derives most naturally from a [4,4] carbon nanotube<sup>4</sup>. I

used the finite-field London theory<sup>5</sup> to calculate its magnetic properties. This theory successfully predicted the magnetic susceptibility of C<sub>60</sub> (refs 6, 7) and C<sub>60</sub><sup>-</sup> (ref. 8).

The toroid has an extremely large and anisotropic ring-current diamagnetic susceptibility,  $\chi_{RC}$  (Table 1). The calculation clearly shows that the preferred current path is around the six-fold axis. The ring-current magnetic susceptibility of C<sub>576</sub> with the field perpendicular to the plane ( $\chi_{RC}^{\perp}$ ) is about four times larger than that of the compara-

bly sized, icosahedral C<sub>540</sub> (which has a ring-current magnetic susceptibility about 13 per cent that of graphite, rotationally averaged, on a per-carbon basis)<sup>3</sup>. Scaling of  $\chi_{RC}^{\perp}$  for toroidal C<sub>576</sub> with respect to icosahedral C<sub>540</sub> gives a value of 2.75, based on the number of  $\pi$ -electrons and the mean-square radius of the electronic circulations.

How can we relate the magnetic properties to the electrical conductivity? Following London<sup>9</sup> we may derive an effective mass ( $m^*$ ) for the  $\pi$ -electrons of these molecules

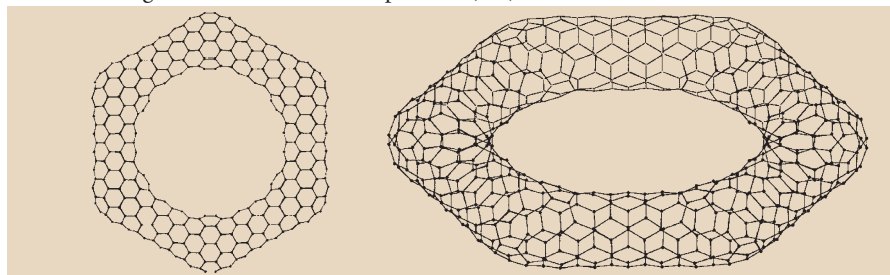


**Figure 1** Two views of the C<sub>576</sub> carbon toroid (after ref. 4).

**Table 1** Calculated  $\pi$ -electron ring-current magnetic properties

Fullerene	$\chi_{RC}$ (relative to benzene) (p.p.m., centre)	$\delta_{RC}^*$
C <sub>60</sub> (I <sub>h</sub> )	-0.5	1.2
C <sub>540</sub> (I <sub>h</sub> )	144.6	-13.3
C <sub>576</sub> (C <sub>6v</sub> , toroid)	657.2 ( $\Delta$ )	-19.6
	22.4 (I)	-1.9

\* $\delta_{RC}$  is the NMR ring-current chemical shift of a central atom.

by scaling the quantum mechanical result with the free-electron value of the magnetic susceptibility. Using a modern parametrization we obtain an effective mass of  $1.5m_e$  for the highest occupied molecular orbital (HOMO) of benzene, whereas a value for the toroid may be obtained from

$$\frac{m^*(C_{576})}{m^*(benzene)} = \frac{\chi_{RC}(benzene)}{\chi_{RC}(C_{576})} \times \frac{\rho^2(C_{576})}{\rho^2(benzene)}$$

$$= \frac{99.8}{4 \times 130.5} = 0.2$$

where  $\rho^2$  is the mean square of the distance of the electronic circulation from the axis of the magnetic field, Z. This is evaluated in the case of the toroid from the atomic coordinates of the carbon atoms:

$$\sum_i^{576} \frac{(x_i^2 + y_i^2)}{576}$$

and thus the area of the toroid in the  $x$ - $y$  plane is about 100 times that of the benzene molecule. The ring-current magnetic susceptibility of the HOMO electrons in the toroid is 130 times larger than the total ring-current magnetic susceptibility of the benzene molecule. Thus  $m^*(C_{576} \text{ HOMO}) = 0.3m_e$ , and because the mobility is usually taken to be inversely proportional to the effective mass we may expect that these carriers will show high conductivities. This is in agreement with the relatively high conductivities measured for linear nanotubes<sup>10-14</sup>.

There has been interest in the change in electronic structure that would occur on passing a magnetic flux quantum through a benzene ring. The strong coupling of some of the toroid energy levels to the magnetic field and the concentration of levels near the energy gap (especially in other toroids), suggests that these objects will provide ideal candidates for magnetically induced changes in electronic structure<sup>15</sup>. At large size, of course, the level distinctions vanish as the  $\pi$ -electron states merge into energy bands and the flux jumps would be observable as the Aharonov-Bohm effect<sup>1</sup>.

**R. C. Haddon**

Departments of Chemistry and Physics,  
University of Kentucky,  
Lexington, Kentucky 40506-0055, USA

1 Liu, J. *et al.* *Nature* **385**, 780-781 (1997).  
2 Haddon, R. C. *J. Am. Chem. Soc.* **100**, 1722-1728 (1978).  
3 Haddon, R. C. *Nature* **378**, 249-255 (1995).  
4 Dunlap, B. I. *Phys. Rev. B* **46**, 1933-1936 (1992).  
5 Elser, V. & Haddon, R. C. *Nature* **325**, 792-794 (1987).  
6 Haddon, R. C. *et al.* *Nature* **350**, 46-47 (1991).  
7 Ruoff, R. S. *et al.* *J. Phys. Chem.* **95**, 3457-3459 (1991).

8. Diederich, J., Gangopadhyay, A. K. & Schilling, J. S. *Phys. Rev. B* **54**, 9662-9665 (1996).  
9. London, F. J. *Phys. Radium (Paris)* **8**, 397-409 (1937).  
10. Langer, L. *et al.* *Phys. Rev. Lett.* **76**, 479-482 (1996).  
11. Dai, H., Wong, E. W. & Lieber, C. M. *Science* **272**, 523-525 (1996).  
12. Ebbesen, T. W. *et al.* *Nature* **382**, 54-56 (1996).  
13. Thess, A. *et al.* *Science* **273**, 483-487 (1996).  
14. Fischer, J. E. *et al.* *Phys. Rev. B* **55**, 4921-4924 (1997).  
15. Haddon, R. C. in *The Chemical Physics of Fullerenes 10 (and 5) Years Later* (ed. Andreoni, W.) 91-98 (Kluwer, Dordrecht, 1996).

## Vision in dim light

On testing my own vision in very dim light I observed two phenomena associated with the lack of retinal rods (the receptors specialized for vision in dim light) in the fovea, the region corresponding to our centre of gaze. First, a bright (or dark) straight line passing through the fovea was seen as discontinuous, with a clear 1° gap. Second, after adapting to dim light conditions, when I blocked light to one eye as far as possible and viewed a brightly lit surface with the other eye, I perceived a swarm of colourless scintillations throughout the visual field of the occluded eye, except for an area about 1° in diameter at the centre of gaze. Each scintillation may represent the simultaneous capture of single quanta by several closely spaced rods.

Damage to a small area of the primary visual cortex produces a circumscribed area of blindness in the visual field, a scotoma, which is not usually apparent as the background fills in the blind area. A straight line crossing through the blind area is generally seen as uninterrupted. This completion phenomenon is also said to occur for lines crossing the normal blind spot produced by the absence of receptors where the optic nerve enters the retina.

The fovea contains cones but no rods. In light that is too dim to activate cones (scotopic conditions) we therefore have a blind spot at the centre of our visual field. I asked whether a line would show a gap when it crossed this foveal scotopic blind spot, or be completed as in the case of a cortical scotoma. On getting up at night I tested this on an abundance of lines, such as the edges of walls, wallpaper designs, and window lattices projected onto walls by street lights. Under these conditions only rods were active (no colours were visible, and any small spots vanished when looked at directly).

I could discern a clear gap when a line passed through the point of fixation. Fixation on a small object is not easy in dim light as the object disappears and gaze tends to wander, but with practice it is possible to fixate on a line so that the gap becomes obvious. Both light lines on a dark background and dark lines on a light background showed a gap as if invaded by the background. Edge boundaries between light and dark areas presented a notch of intermediate brightness. These gaps subtended

about 1° of arc. The corners of a dark or light square were chopped off and similarly replaced by a region of intermediate brightness. In uniformly lit regions, no dark or light spots were seen wandering with shifting gaze. When I fixated on a 12-mm dark spot on patterned wallpaper it disappeared, filled in by the lighter background, and when I viewed a coarsely textured rug I saw a spot of intermediate brightness which wandered to follow my direction of gaze.

I conclude that under conditions of rod vision, line completion does not occur across the foveal scotoma (mentioned in passing in an earlier paper<sup>1</sup>), corners are not filled in, nor are patterns and textures completed. But filling-in does occur across diffusely lit surfaces, both dark and light.

When I get up at night, dark adapted over many hours, there is just enough light for me to make my way around but too little to allow me to find small objects. By cupping a hand lightly over one eye before turning on the lights this nuisance can be avoided, because when the lights are turned off again dark adaptation is fully preserved in the covered eye, though the other eye is temporarily completely blind. In its thickest part my hand attenuates light by 7-8 log units (measured with a Pritchard photometer, Photo Research PR-1980, Chatsworth).

Recently I noticed a curious phenomenon. With the room light on, facing a bright, uniformly lit wall (luminance 1.8 log cd m<sup>-2</sup>), I observed tiny speckles in the dark-adapted covered eye. These bright, colourless points were scattered evenly over the field of view except for an area roughly 1° wide in the centre, and each appeared for a very short time (less than 0.5 s). Their concentration increased dramatically as I let more light into the occluded eye (and tended to be replaced by a wavy, swirling texture), whereas placing two hands over the eye greatly reduced the speckles. They waxed and waned in vividness over a period of many seconds, out of phase with the view seen by the open, light-adapted eye. They were most apparent when I attended to them and faded when attention was switched to the open eye. The variation in brightness is presumably a manifestation of binocular rivalry.

It is well established that the absolute threshold for perception of light is reached when five or more closely spaced rods all capture a quantum of light within a brief period of time<sup>2</sup>. Absolute threshold is commonly estimated at 10<sup>-6</sup> cd m<sup>-2</sup>, a level of darkness that may plausibly be reached by my 7-8-log-unit filter. I suggest that the speckles could represent such coincident threshold events, because they appear at very low light levels, they increase in density as more light is admitted, they are absent in the rod-free part of the retina, and they are colourless. I have no idea why they should occur only when one eye is dark adapted